


Cite this: *RSC Adv.*, 2017, 7, 24674

Enhancement of the near-infrared emission of Ce³⁺–Yb³⁺ co-doped Y₃Al₅O₁₂ phosphors by doping Bi³⁺ ions

K. Santhosh Kumar,^a Chaogang Lou,^a A. Gowri Manohari,^b Cao Huihui^a and Didier Pribat^a

Ce³⁺–Yb³⁺ co-doped Y₃Al₅O₁₂ phosphors are one of most the potential candidates of down-conversion materials for photovoltaic cells. To improve the near-infrared emission from Yb³⁺ ions, Bi³⁺ ions were introduced into the phosphors. The experimental results showed that the intensity of Yb³⁺ emission was greatly enhanced after doping Bi³⁺ ions into the phosphors. This may be attributed to an additional pathway via Bi³⁺ ions for the energy transfer from Ce³⁺ to Yb³⁺. Different from the co-doped phosphors, where the energy of Ce³⁺ ions was transferred only to Yb³⁺ ions, in Bi³⁺–Ce³⁺–Yb³⁺ tri-doped phosphors, the energy of Ce³⁺ ions could be transferred not only to Yb³⁺ ions but also to Bi³⁺ ions. Then, Bi³⁺ ions transferred part of the energy to Yb³⁺ ions. This enabled Yb³⁺ ions to obtain more energy and enhance their near-infrared emission.

Received 11th March 2017
Accepted 22nd April 2017

DOI: 10.1039/c7ra02943h

rsc.li/rsc-advances

Introduction

Crystalline silicon (c-Si) solar cells have quickly developed over the past few decades because of the huge demand for clean energy.^{1,2} One of the factors limiting the conversion efficiency of the solar cells is the spectral mismatch between the solar spectrum and the energy band gap of silicon.^{1,3} This results in the problems that the photons with energies lower than the band gap cannot be absorbed, and the higher-energy photons lose the excess of the energy in the cells through thermalization. A possible solution to the latter problem is to cut a higher-energy photon into two or more near-infrared (NIR) photons, which can still be absorbed by the cells.⁴

A down-conversion process is considered to be a promising way to enhance the efficiency of solar cells because it provides the possibility of converting one higher-energy photon into two or more lower-energy photons.^{5,6} It has been reported that by this way, the maximum conversion efficiency of the c-Si solar cells could be greatly improved.⁴ For this reason, down-conversion materials have attracted significant attention in recent years.^{7–10}

Rare earth (RE) phosphors have been considered as one of the potential candidates of down-conversion materials because RE ions have rich energy level structures, which allow efficient spectral conversion.¹¹ Among RE ions, Yb³⁺ ions are desirable due to their high luminescence quantum efficiency and emitted wavelength (950–1050 nm), which is close to the band gap of

Si.¹² To date, a number of studies have been performed on the RE³⁺–Yb³⁺ co-doped phosphors, in which RE³⁺ ions (RE = Tb, Tm, Pr, Er, Nd, and Ho) were used as sensitizers and Yb³⁺ ions were used as activators.^{13–17} However, the weak and narrow absorption of these sensitizers prevented them from being applied as photovoltaic down-conversion materials.¹⁸

On the other hand, some rare earth ions, such as Ce³⁺ and Eu²⁺, with broader absorption have also been used as sensitizers in the phosphors.^{19–22} Because of the success of Ce³⁺-doped Y₃Al₅O₁₂ (YAG) phosphors in semiconductor lighting, Ce³⁺–Yb³⁺ co-doped Y₃Al₅O₁₂ phosphors have naturally been considered as potential down-conversion materials.¹⁹ Although several attempts have been made in this regard, the efficiency of the energy transfer from Ce³⁺ to Yb³⁺ in the phosphors is still not satisfactory due to the complicated mechanism.^{23,24}

In this study, Bi³⁺ ions were introduced into Ce³⁺–Yb³⁺ co-doped YAG phosphors to improve the energy transfer from Ce³⁺ to Yb³⁺. Their influences on the emission of Yb³⁺ and the energy transfers between Bi³⁺, Ce³⁺, and Yb³⁺ were studied.

Experimental

Bi³⁺–Ce³⁺–Yb³⁺ tri-doped YAG phosphors were prepared by a traditional solid-state reaction method. The powders of Y₂O₃ (99.99%), Al₂O₃ (99.99%), Bi₂O₃ (99%), Ce₂O₃ (99.99%), and Yb₂O₃ (99.99%) were stoichiometrically mixed. Then, the mixture was transferred into an alumina crucible and heated at 1600 °C for 6 h in an N₂ + H₂ atmosphere in a chamber furnace. The samples were cooled down to room temperature and were ground again. The excitation and emission spectra of the phosphors were obtained using Ocean Optics MAYA 2000PRO. Fluorescence lifetimes were measured using a FM-4P-TCSPC

^aSchool of Electronic Science and Engineering, Southeast University, Nanjing 210096, Jiangsu Province, People's Republic of China. E-mail: lcg@seu.edu.cn

^bSchool of Biological Sciences and Medical Engineering, Southeast University, Nanjing 210096, Jiangsu Province, People's Republic of China



spectrofluorometer (Horiba Jobin Yvon). All the measurements were carried out at room temperature.

Results and discussion

Fig. 1 shows the emission spectra of $\text{Y}_{3-x-y-z}\text{Al}_5\text{O}_{12} : x\text{Bi}^{3+}, y\text{Ce}^{3+}, z\text{Yb}^{3+}$ ($x = 0, 0.03; y = 0.01$; and $z = 0.05, 0.1, 0.15, 0.2$, and 0.25) phosphors under an excitation of 455 nm. It can be seen that the emissions from Ce^{3+} and Yb^{3+} vary with the Yb^{3+} concentration. When Yb^{3+} concentration was low ($z = 0.05, 0.1$, and 0.15), the NIR emission from Yb^{3+} ions increased with an increase in the Yb^{3+} concentration. This occurred because the energy transferred to Yb^{3+} from Ce^{3+} increased with the concentration of Yb^{3+} . This is also the reason why the emission from Ce^{3+} ions decreased with the increasing Yb^{3+} concentration. When the Yb^{3+} concentration continued to increase to $z = 0.2$ and 0.25 , although the energy from Ce^{3+} to Yb^{3+} increased, the Yb^{3+} emission became weaker due to the concentration quenching effect of Yb^{3+} .²⁵

The most desirable result, as shown in Fig. 1, is that in the cases of $x = 0.03, y = 0.01$, and $z = 0.05, 0.10$, and 0.15 , the intensity of NIR emission from Yb^{3+} ions in $\text{Bi}^{3+}\text{-Ce}^{3+}\text{-Yb}^{3+}$ tri-doped phosphors was stronger than that in $\text{Ce}^{3+}\text{-Yb}^{3+}$ co-doped phosphors ($x = 0, y = 0.01$, and $z = 0.1$). Fig. 2 shows the

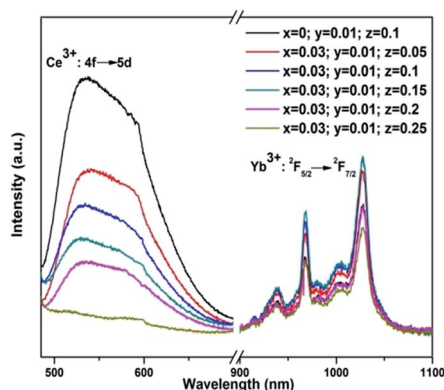


Fig. 1 The emission spectra of different YAG phosphors under the excitation of 455 nm.

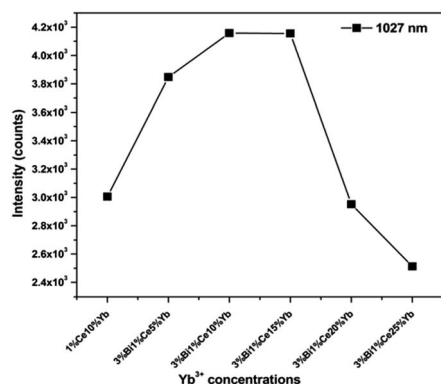


Fig. 2 Emission intensities of Yb^{3+} at 1027 nm from different YAG phosphors under the excitation of 455 nm.

intensities of the emissions at 1027 nm from the phosphors with different chemical compositions. Although the NIR emission of the tri-doped samples when $z = 0.2$ and 0.25 was weaker than that of the co-doped phosphors due to the concentration quenching effect of Yb^{3+} , the stronger emission of the tri-doped phosphors when $z = 0.05, 0.10$, and 0.15 indicated that the introduction of Bi^{3+} ions could improve the emission from Yb^{3+} ions.

Because Yb^{3+} ions cannot absorb the photons with a wavelength of 455 nm, their emission resulted from the energy transfer inside the phosphors. To explain the curves shown in Fig. 1 and 2, it is necessary to clarify the energy transfers between Bi^{3+} , Ce^{3+} , and Yb^{3+} ions in the tri-doped phosphors. Fig. 3 shows the luminescence decay curves of Ce^{3+} (monitored at 560 nm) in singly Ce^{3+} -doped ($x = 0, y = 0.01$, and $z = 0$), $\text{Ce}^{3+}\text{-Yb}^{3+}$ co-doped ($x = 0, y = 0.01$, and $z = 0.1$), and $\text{Bi}^{3+}\text{-Ce}^{3+}\text{-Yb}^{3+}$ tri-doped ($x = 0.03, y = 0.01$, and $z = 0.05, 0.1, 0.15$, and 0.2) YAG phosphors under the excitation of 455 nm. Clearly, the emission from Ce^{3+} in the tri-doped phosphors decayed faster than that in the $\text{Ce}^{3+}\text{-Yb}^{3+}$ co-doped phosphors. Because the tri-doped samples have Bi^{3+} ions, whereas the co-doped sample does not, the faster decay of the emission from Ce^{3+} in the tri-doped phosphors might be attributed to the energy transfer from Ce^{3+} ions to Bi^{3+} ions.

To understand the energy transfer in detail, the efficiency of the energy transfers from Ce^{3+} to other ions was calculated. According to previous studies,^{26,27} the energy transfer efficiency η_{ETE} can be estimated using the following equation:

$$\eta_{\text{ETE}} = 1 - \frac{\tau_{\text{R}}}{\tau_{\text{R0}}} \quad (1)$$

where τ_{R0} is the fluorescence lifetime of the donor (sensitizer) in the absence of acceptors (activators) and τ_{R} is the fluorescence lifetime of the donor in the presence of acceptors. The fluorescence lifetime can be obtained using the following equation:^{20,28}

$$\tau = \frac{\int_0^{\infty} tI(t)dt}{\int_0^{\infty} I(t)dt} \quad (2)$$

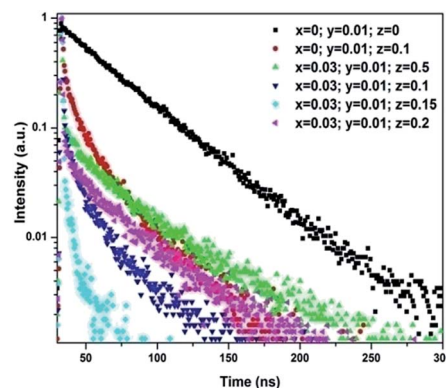


Fig. 3 The decay curves of Ce^{3+} emission at 560 nm for YAG phosphors under an excitation of 455 nm.



where $I(t)$ represents the luminescence intensity at time t .

From the decay curves shown in Fig. 3, the fluorescence lifetimes of Ce^{3+} were calculated to be 15.3 ns in the tri-doped phosphors ($x = 0.03$, $y = 0.01$, and $z = 0.1$), 24.3 ns in Ce^{3+} – Yb^{3+} co-doped phosphors ($x = 0$, $y = 0.01$, and $z = 0.1$), and 65.7 ns in the singly Ce^{3+} -doped phosphors ($x = 0$, $y = 0.01$, and $z = 0$). The energy transfer efficiency calculated from the decay curve of Ce^{3+} in the tri-doped phosphors was about 76.78%, whereas the energy transfer efficiency in the co-doped phosphors was 63.02%.

The reasonable explanation for the different energy transfer efficiencies in the two types of phosphors was that in the co-doped phosphors, there was only one pathway for the energy transfer. The energy was transferred from Ce^{3+} to Yb^{3+} , whereas in the tri-doped phosphors, the energy of Ce^{3+} could be transferred *via* two pathways. One pathway was from Ce^{3+} to Yb^{3+} and the other was from Ce^{3+} to Bi^{3+} to Yb^{3+} .

The evidence for the energy transfer from Ce^{3+} to Bi^{3+} can be found in Fig. 4, which shows the decay curves of Ce^{3+} singly doped and Ce^{3+} – Bi^{3+} co-doped YAG phosphors. Under the excitation of 455 nm, the emission of Ce^{3+} in the singly doped phosphors showed nearly a single exponential decay with a fluorescence lifetime of 65.7 ns, whereas in Ce^{3+} – Bi^{3+} co-doped samples, the fluorescence lifetime decreased to 56.3 ns. The calculated energy transfer efficiency was 14.31%. This indicated that the energy transfer from Ce^{3+} to Bi^{3+} was possible inside the phosphors.

After Bi^{3+} ions received energy from Ce^{3+} , the energy could be partly transferred to Yb^{3+} . To prove this, the Bi^{3+} singly doped and Bi^{3+} – Yb^{3+} co-doped YAG phosphors were prepared. The evidence of the energy transfer from Bi^{3+} to Yb^{3+} can be found in Fig. 5 and 6. From Fig. 5(a), it can be seen that an excitation band is centered at 275 nm due to the transition of Bi^{3+} : $^1\text{S}_0 \rightarrow ^1\text{P}_1$, $^3\text{P}_1$ detected by monitoring at 304 and 460 nm. Moreover, a similar excitation spectrum was also obtained for the transition of Yb^{3+} : $^2\text{F}_{5/2} \rightarrow ^2\text{F}_{7/2}$ at the monitoring wavelength of 1028 nm. The similarity in the shape of both excitation spectra can be considered as a direct evidence for the energy transfer (ET) from Bi^{3+} to Yb^{3+} . The emission spectra of singly doped Bi^{3+}

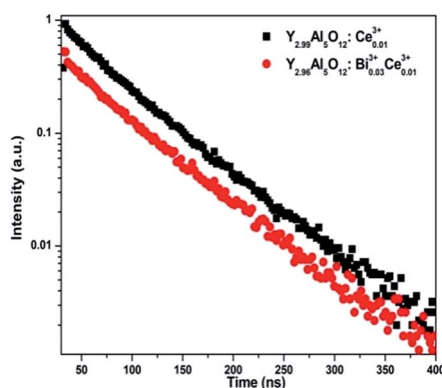


Fig. 4 The decay curves of Ce^{3+} emission at 560 nm for Ce^{3+} singly doped and Ce^{3+} – Bi^{3+} co-doped YAG phosphors under an excitation of 455 nm.

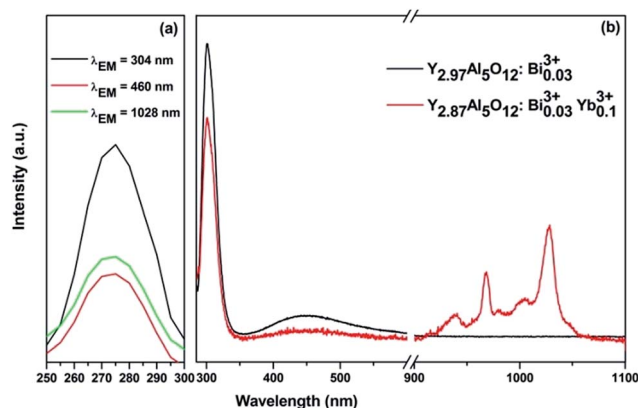


Fig. 5 (a) Excitation spectra of $\text{Y}_{2.87}\text{Al}_5\text{O}_{12}:\text{Bi}_{0.03}^{3+}\text{Ce}_{0.1}^{3+}$ monitored at the emission wavelengths of 304 nm, 460 nm, and 1028 nm and (b) emission spectra of Bi^{3+} singly doped and Bi^{3+} – Yb^{3+} co-doped YAG phosphors under an excitation wavelength of 275 nm.

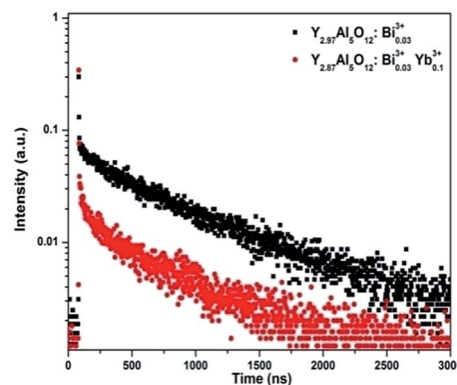


Fig. 6 The decay curves of Bi^{3+} emission at 304 nm for Bi^{3+} singly doped and Bi^{3+} – Yb^{3+} co-doped YAG phosphors under an excitation of 275 nm.

and co-doped Bi^{3+} – Yb^{3+} phosphors under the excitation of 275 nm are shown in Fig. 5(b). The singly doped Bi^{3+} spectrum depicts two emission peaks centered at 304 nm and 460 nm. In the co-doped Bi^{3+} – Yb^{3+} samples, apart from the emissions of Bi^{3+} ions, a strong NIR emission of Yb^{3+} could also be obtained at 1028 nm, which was accompanied by several weak shoulder peaks due to the transitions among different Stark levels of $^2\text{F}_j$ ($j = 5/2, 7/2$) in Yb^{3+} . Because Yb^{3+} ions cannot absorb the photons of 275 nm, their NIR emission indicates an energy transfer from Bi^{3+} to Yb^{3+} .

Fig. 6 shows the decay curves of singly Bi^{3+} doped and Bi^{3+} – Yb^{3+} co-doped phosphors under an excitation of 275 nm. The faster decay of Bi^{3+} emission in the co-doped samples also proved the energy transfer from Bi^{3+} to Yb^{3+} . From Fig. 6, the fluorescence lifetime of Bi^{3+} was calculated as 768 ns in the singly doped phosphors, decreased to 576 ns after Yb^{3+} ions were introduced. The calculated energy transfer efficiency from Bi^{3+} to Yb^{3+} was 24.95%.

In principle, the amount of the energy transferred from Ce^{3+} to Yb^{3+} in the tri-doped phosphors should be close to that in



Ce^{3+} – Yb^{3+} co-doped phosphors because these two types of phosphors have the same concentrations of Ce^{3+} and Yb^{3+} .²⁹ This should result in similar intensities in the NIR emission from Yb^{3+} . However, in the tri-doped phosphors, besides transferring energy to Yb^{3+} , Ce^{3+} could also transfer energy to Bi^{3+} . The energy transferred to Bi^{3+} was then partly transferred to Yb^{3+} ; thus, Yb^{3+} ions obtained more energy in the tri-doped phosphors than in the co-doped phosphors. This is why the NIR emission from Yb^{3+} in the tri-doped phosphors was stronger than that in the co-doped phosphors, as shown in Fig. 1.

Based on the abovementioned results, the possible energy transfer processes were analyzed, and the schematic energy level diagram is shown in Fig. 7. In the Ce^{3+} – Bi^{3+} – Yb^{3+} tri-doped phosphors, the possible energy transfer processes takes place in four ways: $\text{Ce}^{3+} \rightarrow \text{Yb}^{3+}$, $\text{Ce}^{3+} \rightarrow \text{Bi}^{3+}$, $\text{Bi}^{3+} \rightarrow \text{Yb}^{3+}$, and $\text{Ce}^{3+} \rightarrow \text{Bi}^{3+} \rightarrow \text{Yb}^{3+}$. For the first energy transfer of $\text{Ce}^{3+} \rightarrow \text{Yb}^{3+}$, the energy of the $5d \rightarrow 4f$ transition of Ce^{3+} was approximately twice as high as the energy of the $^2\text{F}_{5/2} \rightarrow ^2\text{F}_{7/2}$ transition of Yb^{3+} . The energy of Ce^{3+} transferred to Yb^{3+} by two possible ways. One way was that one UV/blue photon was converted into two NIR photons by a cooperative energy transfer (CET),³⁰ other was that the energy transferred from Ce^{3+} to Yb^{3+} via a charge transfer state (CTS).^{24,31,32} To date, both CTS and CET models lack direct experimental evidence and are still in dispute. For the second energy transfer process of $\text{Ce}^{3+} \rightarrow \text{Bi}^{3+}$, the mechanism was more complicated. The electrons of the excited $5d$ state of Ce^{3+} ions could transit to the $^3\text{P}_2$ state of Bi^{3+} ions because these two energy levels were close to each other. On the other hand, after Bi^{3+} ions obtain the energy, part of electrons of the excited $^3\text{P}_2$ state of Bi^{3+} ions could transit back to $5d$ state of Ce^{3+} ions, and rest of the electrons transited to $^2\text{F}_{5/2}$ level of Yb^{3+} or the ground state $^1\text{S}_0$ of Bi^{3+} . For the third energy transfer of $\text{Bi}^{3+} \rightarrow \text{Yb}^{3+}$, the energy level $^3\text{P}_1$ of Bi^{3+} was approximately twice as high as the energy difference between the $^2\text{F}_{5/2}$ and $^2\text{F}_{7/2}$ levels of Yb^{3+} . The energy of Bi^{3+} might directly transfer to nearby Yb^{3+} ions via CET.³³ On the basis of the abovementioned ET processes, the fourth energy transfer of $\text{Ce}^{3+} \rightarrow \text{Bi}^{3+} \rightarrow \text{Yb}^{3+}$ is easy to be understood. At an excitation of 455 nm, after Ce^{3+} ions were excited to the $5d$ state, part of the excited electrons transited to the $^2\text{F}_{5/2}$ and $^2\text{F}_{7/2}$ states of Ce^{3+} , and part of the excited electrons transited to the ^3P states of Bi^{3+} ions and then Bi^{3+} transferred energy to Yb^{3+} .

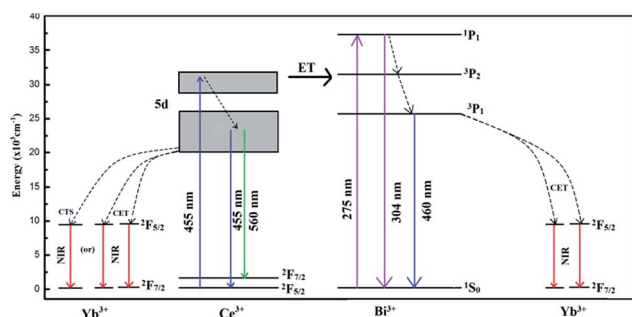


Fig. 7 Schematic energy level diagram of Ce^{3+} – Bi^{3+} – Yb^{3+} tri-doped $\text{Y}_3\text{Al}_5\text{O}_{12}$ phosphors.

According to the above mentioned ET processes, Bi^{3+} ions, as the new pathway for the energy transfer, played an important role in enhancing the NIR emission of Ce^{3+} – Bi^{3+} – Yb^{3+} tri-doped $\text{Y}_3\text{Al}_5\text{O}_{12}$ phosphors.

Note that the enhancement of NIR emission from Yb^{3+} by introducing Bi^{3+} ions into Ce^{3+} – Yb^{3+} co-doped phosphors does not mean that other ions have similar effects. We attempted to dope Tb^{3+} ions into Ce^{3+} – Yb^{3+} co-doped phosphors, but did not observe an improvement in Yb^{3+} emission. Therefore, clarifying the mechanism of the energy transfer in the Bi^{3+} – Ce^{3+} – Yb^{3+} YAG phosphors is important to further improve the NIR emission in future studies.

Conclusions

The NIR emission from Yb^{3+} in Ce^{3+} – Yb^{3+} co-doped $\text{Y}_3\text{Al}_5\text{O}_{12}$ phosphors under an excitation of 455 nm was improved by introducing Bi^{3+} ions. This was because Ce^{3+} ions transferred energy to Bi^{3+} ions in addition to Yb^{3+} ions in Bi^{3+} – Ce^{3+} – Yb^{3+} tri-doped YAG phosphors. Then, the energy of Bi^{3+} ions was partly transferred to Yb^{3+} ions. This made Yb^{3+} ions obtain more energy in the tri-doped phosphors than in the co-doped phosphors and resulted in more NIR emission.

Acknowledgements

The authors thank the support provided by the Natural Science Foundation of Jiangsu (Grant No. BK2011033), Jiangsu Planned Projects for Postdoctoral Research Funds (Grant No. 1501042B) and the Primary Research & Development Plan of Jiangsu Province (Grant No. BE2016175). The authors also thank Dr Xuefeng Ge at the Center for Analysis and Testing of Nanjing Normal University for his help in characterizing the decay curves of the phosphors.

References

- 1 B. M. van der Ende, L. Aarts and A. Meijerink, *Adv. Mater.*, 2009, **21**, 3073.
- 2 B. Fan, C. Chlique, O. Merdrignac-Conanec, X. H. Zhang and X. P. Fan, *J. Phys. Chem. C*, 2012, **116**, 11652.
- 3 B. van der Zwaan and A. Rabl, *Sol. Energy*, 2003, **74**, 19.
- 4 T. Trupke, M. A. Green and P. Würfel, *J. Appl. Phys.*, 2002, **92**, 1668.
- 5 W. Shockley and H. J. Queisser, *J. Appl. Phys.*, 1961, **32**, 510.
- 6 B. S. Richards, *Sol. Energy Mater. Sol. Cells*, 2006, **90**, 1189.
- 7 D. C. Yu, S. Ye, M. Y. Peng, Q. Y. Zhang and L. Wondraczek, *Appl. Phys. Lett.*, 2012, **100**, 191911.
- 8 X. Wei, S. Huang, Y. Chen, C. Guo, M. Yin and W. Xu, *J. Appl. Phys.*, 2010, **107**, 103107.
- 9 J. J. Eilers, D. Biner, J. T. van Wijngaarden, K. Kramer, H. U. Gudel and A. Meijerink, *Appl. Phys. Lett.*, 2010, **96**, 151106.
- 10 H. Zhang, J. Chen and H. Guo, *J. Rare Earths*, 2011, **29**, 822.
- 11 R. Zhou, Y. Kou, X. Wei, C. Duan, Y. Chen and M. Yin, *Appl. Phys. B*, 2012, **107**, 483.
- 12 Q. Y. Zhang and X. Y. Huang, *Prog. Mater. Sci.*, 2010, **55**, 353.



- 13 P. Vergeer, T. J. H. Vlugt, M. H. F. Kox, M. I. den Hertog, J. P. J. M. van der Eerden and A. Meijerink, *Phys. Rev. B: Condens. Matter Mater. Phys.*, 2005, **71**, 014119.
- 14 Q. Y. Zhang, C. H. Yang and Y. X. Pan, *Appl. Phys. Lett.*, 2007, **90**, 021107.
- 15 D. Q. Chen, Y. S. Wang, Y. L. Yu, P. Huang and F. Y. Weng, *Opt. Lett.*, 2008, **33**, 1884.
- 16 B. M. van der Ende, L. Aarts and A. Meijerink, *Phys. Chem. Chem. Phys.*, 2009, **11**, 11081.
- 17 J. M. Meijerink, L. Aarts, B. M. van der Ende, T. J. H. Vlugt and A. Meijerink, *Phys. Rev. B: Condens. Matter Mater. Phys.*, 2010, **81**, 035107.
- 18 J. Ueda and S. Tanabe, *J. Appl. Phys.*, 2009, **106**, 043101.
- 19 Y. Li, J. Wang, W. Zhou, G. Zhang, Y. Chen and Q. Su, *Appl. Phys. Express*, 2013, **6**, 082301.
- 20 X. Liu, Y. Teng, Y. Zhuang, J. Xie, Y. Qiao, G. Dong, D. Chen and J. Qiu, *Opt. Lett.*, 2009, **34**, 3565.
- 21 J. Sun, Y. Sun, J. Zeng and H. Du, *Opt. Mater.*, 2013, **35**, 1276.
- 22 G. Gao and L. Wondraczek, *J. Mater. Chem. C*, 2013, **1**, 1952.
- 23 E. van der Kolk, O. M. Ten Kate, J. W. Wiegman, D. Biner and K. W. Kramer, *Opt. Mater.*, 2011, **33**, 1024.
- 24 D. C. Yu, F. T. Rabouw, W. Q. Boon, T. Kieboom, S. Ye, Q. Y. Zhang and A. Meijerink, *Phys. Rev. B: Condens. Matter Mater. Phys.*, 2014, **90**, 165126.
- 25 J. Liao, Y. Lin, Y. Chen, Z. Luo, E. Ma, X. Gong, Q. Tan and Y. Huang, *J. Opt. Soc. Am. B*, 2006, **23**, 2572.
- 26 P. I. Paulose, G. Jose, V. Thomas, N. V. Unnikrishnan and M. K. R. Warriar, *J. Phys. Chem. Solids*, 2003, **64**, 841.
- 27 Q. Y. Zhang, C. H. Yang, Z. H. Jiang and X. H. Ji, *Appl. Phys. Lett.*, 2007, **90**, 061914.
- 28 A. Speghini, M. Bettinelli, P. Riello, S. Bucella and A. Benedetti, *J. Mater. Res.*, 2005, **20**, 2780.
- 29 L.-M. Shao and X.-P. Jing, *ECS J. Solid State Sci. Technol.*, 2012, **1**, R22.
- 30 H. Lin, S. M. Zhou, H. Teng, Y. K. Li, W. J. Li, X. R. Hou and T. T. Jia, *J. Appl. Phys.*, 2010, **107**, 043107.
- 31 J. Zhao, C. Guo, T. Li, D. Songa and X. Su, *Phys. Chem. Chem. Phys.*, 2015, **17**, 26330.
- 32 J. Zhao, C. Guo and T. Li, *RSC Adv.*, 2015, **5**, 28299.
- 33 C. Parthasaradhi Reddy, V. Naresh, B. Chandra Babu and S. Buddhudu, *Adv. Mater. Phys. Chem.*, 2014, **4**, 165.

